

MYELOID NEOPLASIA

A PML/RAR α direct target atlas redefines transcriptional deregulation in acute promyelocytic leukemia

Yun Tan,^{1,*} Xiaoling Wang,^{1,2,*} Huan Song,^{1,*} Yi Zhang,¹ Rongsheng Zhang,^{1,2} Shufen Li,¹ Wen Jin,¹ Saijuan Chen,¹ Hai Fang,¹ Zhu Chen,^{1,3} and Kankan Wang¹⁻³

¹Shanghai Institute of Hematology, State Key Laboratory of Medical Genomics, National Research Center for Translational Medicine at Shanghai, Ruijin Hospital Affiliated to Shanghai Jiao Tong University School of Medicine, Shanghai, China; ²School of Life Sciences and Biotechnology, Shanghai Jiao Tong University, Shanghai, China; and ³Sino-French Research Center for Life Sciences and Genomics, Ruijin Hospital, Shanghai Jiao Tong University School of Medicine, Shanghai, China

KEY POINTS

- An atlas of PML/RAR α direct targets redefines the activating function and explains synergism of all-trans retinoic acid/arsenic trioxide.
- PML/RAR α activates target gene *GFI1* through chromatin conformation at the super-enhancer region, which is required for APL cell growth.

Transcriptional deregulation initiated by oncogenic fusion proteins plays a vital role in leukemia. The prevailing view is that the oncogenic fusion protein promyelocytic leukemia/retinoic acid receptor- α (PML/RAR α), generated by the chromosome translocation t(15;17), functions as a transcriptional repressor in acute promyelocytic leukemia (APL). Here, we provide rich evidence of how PML/RAR α drives oncogenesis through both repressive and activating functions, particularly the importance of the newly identified activation role for the leukemogenesis of APL. The activating function of PML/RAR α is achieved by recruiting both abundant P300 and HDAC1 and by the formation of super-enhancers. All-trans retinoic acid and arsenic trioxide, 2 widely used drugs in APL therapy, exert synergistic effects on controlling super-enhancer-associated PML/RAR α -regulated targets in APL cells. We use a series of in vitro and in vivo experiments to demonstrate that PML/RAR α -activated target gene *GFI1* is necessary for the maintenance of APL cells and that PML/RAR α , likely oligomerized, transactivates *GFI1* through chromatin conformation at the super-enhancer region. Finally, we profile *GFI1* targets and reveal the interplay between *GFI1* and PML/RAR α on chromatin in coregulating target genes. Our study provides

genomic insight into the dual role of fusion transcription factors in transcriptional deregulation to drive leukemia development, highlighting the importance of globally dissecting regulatory circuits. (*Blood*. 2021;137(11):1503-1516)

Introduction

In genetics of myeloid neoplasia, chromosomal translocations often involve transcription factors (TFs), leading to oncogenic fusion TFs that can induce malignant transformation through aberrant transcriptional programs.¹ Depending on the predominant transcriptional activity on direct target genes, these fusion TFs are dichotomously classified as either activators or repressors. This concept of dichotomy has been challenged by the discovery of versatile roles of transcriptional regulators in gene expression,² largely propelled by rapid advances in high-throughput genomic technologies.

Acute promyelocytic leukemia (APL) is characterized by a specific t(15;17) chromosome translocation, which generates the promyelocytic leukemia/retinoic acid receptor- α (PML/RAR α) fusion gene. The encoded fusion protein has been long viewed as a transcriptional repressor of RAR α signaling to interfere with myeloid differentiation.³ Our previous studies have revealed that PML/RAR α can also exert repressive effects on PU.1 target genes.^{4,5} Such repression is largely achieved by the recruitment

of corepressors.^{3,6} However, gene expression profiling has implicated the capacity to upregulate (in addition to downregulate) gene expression, as observed in both PML/RAR α -overexpressed cells and transgenic mice.^{7,8} PML/RAR α can directly transactivate the expression of genes essential for APL pathogenesis.^{9,10} However, only a few such genes have been reported, and the mechanism by which PML/RAR α mediates transcriptional activation on a genome scale is unknown.

TF-governing gene regulation is principally modeled as the switch between 2 mutually exclusive classes of coregulators, coactivators and corepressors, respectively activating and repressing transcription.¹¹ However, this classical model has been challenged by genome-wide binding data of coregulators. In human T cells, both coactivators and corepressors can colocalize on actively transcribed regions.² In embryonic stem cells, the repressor complex and the mediator activator complex are recruited to super-enhancer regions with histone hyperacetylation.¹² These findings suggest a functional interplay between coactivators and corepressors on chromatin.

Current knowledge of corepressors involved in PML/RAR α -mediated transcriptional repression is largely learned from wild-type RAR α .^{3,13} However, we have shown that RAR α -bound canonical retinoic acid responsive elements only account for a small portion of PML/RAR α binding sites.⁴ A more interesting observation is that PML/RAR α tends to bind open chromatin rather than compact chromatin.¹⁴ These observations strongly suggest that PML/RAR α may have distinct coregulator patterns that differ from RAR α . However, the limited information regarding direct targets and coregulators has long hampered our understanding of PML/RAR α -mediated transcriptional de-regulation in APL.

In this study, we established 2 distinct classes of PML/RAR α direct targets that were divergent in function during leukemogenesis: repressed and activated genes. Profiling coregulators (HDAC1 and P300) and histone modifications (H3K4me1 and H3K27ac) allowed us to identify super-enhancer-associated PML/RAR α -regulated target genes for which expression changes were therapeutically relevant, including the target gene, *GFI1*.

GFI1 is a transcriptional regulator with context-dependent roles in hematopoiesis and leukemogenesis.^{15–23} Reduced or loss of *GFI1* expression has been reported in myeloid malignancies,^{18–21} while high *GFI1* expression has been observed in AML1-ETO-positive acute myeloid leukemia (AML)²³ and acute lymphoid leukemia,²² but without clear roles defined for GFI1 in APL pathogenesis. Here, we demonstrate that transactivation of *GFI1* by PML/RAR α (likely oligomerized) and its chromatin conformation regulation at the super-enhancer are necessary for the maintenance of APL. Further profiling GFI1 targets allowed us to identify coregulated genes with PML/RAR α .

Methods

Primary samples and cell lines

Primary APL blasts were obtained according to the Declaration of Helsinki at disease onset from bone marrow of 7 newly diagnosed patients with >85% abnormal promyelocytic blasts (supplemental Table 1, available on the *Blood* Web site). Informed consent was obtained according to procedures approved by the Institutional Review Board from Ruijin Hospital, which is affiliated with Shanghai Jiao Tong University School of Medicine. NB4, U937, and HEK-293T cells were authenticated. Details are available in supplemental Methods.

Identification of PML/RAR α direct targets

The integrative assays of chromatin immunoprecipitation sequencing (ChIP-seq) and RNA sequencing (RNA-seq) were performed on NB4 cells without the treatment of all-*trans* retinoic acid (ATRA) to identify target genes both bound and regulated by PML/RAR α . This integration aimed to minimize possible effects associated with each assay, for example, the influence by the changing state of cells upon PML/RAR α knockdown. MACS suite²⁴ was used to call ChIP-seq binding peaks ($P < 1 \times 10^{-10}$), and edgeR²⁵ was used to identify differentially expressed genes upon short hairpin RNA (shRNA)-mediated PML/RAR α knockdown (false discovery rate <0.01 and at least twofold changes) for 3 days. The maximum distance (50 kb) was used to associate each binding peak with the nearest differential gene showing increased expression (ie, PML/RAR α

directly repressed targets) or decreased expression (ie, PML/RAR α directly activated targets). Details are available in supplemental Methods.

Sequential ChIP (Re-ChIP), chromatin conformation capture (3C), knockdown experiments, luciferase reporter assays, coimmunoprecipitation, and functional experiments

Primers used for these experimental assays are listed in supplemental Table 2, and details are available in supplemental Methods.

Mouse studies

Mouse experiments were carried out in accordance with institutional animal protocols, approved by the Institutional Animal Care and Use Committee of Ruijin Hospital/Shanghai Jiao Tong University School of Medicine. The transplantable murine APL mice model was used in the functional studies of *Gfi1* and the xenograft nonobese diabetic/severe combined immunodeficiency (NOD/SCID) mouse model used to investigate the effects of the intronic enhancer of *GFI1*. Details are available in supplemental Methods.

Bioinformatic and statistical analysis

Bioinformatic and statistical analysis are detailed in supplemental Methods.

Results

PML/RAR α exerts both repressive and activating functions through direct binding

Identification of bona fide direct targets is essential to investigate the oncogenic activity of PML/RAR α during APL pathogenesis. We first sought to identify genes both bound and regulated by PML/RAR α in APL cells through integrative assays of ChIP-seq and RNA-seq (Figure 1A). Briefly, we performed ChIP-seq analysis of NB4 cells, an APL patient-derived cell line, using the antibody against the fusion site of PML/RAR α (supplemental Figure 1A–C). A total of 6415 PML/RAR α binding sites were obtained (supplemental Figure 1D and supplemental Table 3) and confirmed by ChIP-seq data using both anti-RAR α and anti-PML antibodies, which were performed by ourselves and retrieved from previously published data²⁶ (supplemental Figure 1E–F). In parallel, we conducted 2 independent RNA-seq experiments on NB4 cells upon PML/RAR α knockdown using the fusion gene-specific shRNA (supplemental Figure 2A–C) for 3 days, with a total of 2052 PML/RAR α differentially regulated genes identified (supplemental Table 4). PML/RAR α knockdown decreased its binding on chromatin (supplemental Figure 2D) and induced differentiation and apoptosis of NB4 cells (supplemental Figure 2E–I). These effects show similarities to those observed when NB4 cells are treated with arsenic trioxide (ATO).^{3,27} Combining evidence from ChIP-seq and RNA-seq data, we created an atlas of 787 PML/RAR α direct genes, including 363 repressed genes (as expected) and 424 activated genes (unexpected) (Figure 1A; supplemental Table 5). Data from ChIP-quantitative polymerase chain reaction (ChIP-qPCR) using antibodies against the PML moiety, the RAR α moiety, or the fusion site of PML/RAR α supported the existence of 2 classes of PML/RAR α direct targets in APL cells, including both NB4 (supplemental Figure 3) and primary blast cells (Figure 1B).

Furthermore, luciferase reporter assays in U937 transfected with PML/RAR α and in NB4 cells with PML/RAR α knockdown confirmed that transrepression or transactivation was directly mediated by PML/RAR α (Figure 1C; supplemental Table 6).

We next investigated the disease relevance of these 2 classes of PML/RAR α direct targets. Gene set enrichment analysis (GSEA) using RNA-seq data of 179 AML patients (16 APL and 163 non-APL AML)²⁸ revealed that repressed targets were more likely downregulated in APL, while activated genes tended to be enriched among genes highly expressed in APL (Figure 1D). Similar results were obtained when comparing APL samples and normal promyelocytes²⁹ (Figure 1D), suggesting that both classes of PML/RAR α targets were APL specific and malignant related. We also found that these 787 PML/RAR α direct genes were collectively informative to distinguish APL patients from non-APL AML patients and normal promyelocytes (supplemental Figure 4). Furthermore, we also analyzed gene signatures for myeloid differentiation stages, including hematopoietic stem cells, myeloid progenitors, and their mature progeny.^{30,31} We found that PML/RAR α -repressed targets tended to be uniquely expressed in the mature myeloid progeny, ie, band cells and polymorphonuclear neutrophils, consistent with inhibition of terminal neutrophil differentiation by PML/RAR α . Interestingly, PML/RAR α -activated targets were mostly correlated with genes uniquely expressed in promyelocytes and granulocyte/monocyte progenitors (Figure 1E), suggesting the necessity of PML/RAR α in dictating myeloid commitment and the promyelocytic phenotype. We found numerous previously unreported PML/RAR α -activated direct targets, including those critical in hematopoiesis and leukemogenesis, such as GF11, MPO (a strong diagnostic marker for APL³²), and WT1 and MYC (involved in leukemogenesis^{33,34}).

Repressive and activating functions of PML/RAR α are attributed to distinct HDAC1 and P300 binding patterns

Next, we explored potential factors determining the PML/RAR α -mediated transcriptional consequence (activation vs repression). We speculated that PML/RAR α -activated and repressed targets might have different binding patterns of coregulators, considering 2 observations: (1) the recruitment of corepressors is widely recognized to inhibit transcription, whereas the binding of coactivators activates target genes^{3,6}; and (2) the potential of PML/RAR α repressing or activating transcription depends on specific contexts (eg, PML/RAR α may repress the transcription through recruiting corepressors, and ATRA can reactivate the transcription through replacing corepressors with coactivators).³ To test our speculation, we performed ChIP-seq analysis of corepressor HDAC1 and coactivator P300 in NB4 cells to determine chromatin co-occupancy with PML/RAR α (supplemental Tables 7 and 8). We unexpectedly found that both HDAC1 and P300 co-localized with PML/RAR α at the majority of PML/RAR α binding sites in NB4 cells (Figure 2A). Moreover, we found that binding signals of both coregulators were abundant on the PML/RAR α -activated regions, whereas only abundant HDAC1 signals observed on repressed targets (Figure 2B-C). This finding was validated by ChIP-qPCR in primary APL samples (Figure 2D). We also performed co-IP and re-ChIP assays to explore whether HDAC1 and P300 physically bind to PML/RAR α and found that the 3 proteins interacted each other on the chromatin of PML/RAR α targets (Figure 2E-F).

HDAC1 and P300 are generally assumed to be counterplayers that can control histone acetylation levels determining transcriptional repression or activation.³⁵ The coexistence of HDAC1 and P300 on PML/RAR α targets prompted us to further profile the histone acetylation mark H3K27ac. Indeed, the H3K27ac signals on PML/RAR α -activated genes were more significantly abundant than on repressed genes (Figure 2G). Histone hyperacetylation is associated with active chromatin.³⁶ We next quantified the degree of active transcription at PML/RAR α targets by the traveling ratio, defined as the density of RNA polymerase II (Pol II) at the gene body vs near the promoter.³⁷ Indeed, the traveling ratio was significantly higher on PML/RAR α -activated targets than on repressed genes (Figure 2H), indicating that PML/RAR α -activated genes were more actively transcribed in APL.

PML/RAR α transactivates target genes largely through super-enhancer regulation

The interaction between PML/RAR α and P300 on activated targets suggested the involvement of PML/RAR α in enhancer regulation. We thus performed ChIP-seq using the enhancer marks H3K4me1 and H3K27ac to define enhancer regions and found that ~40% of PML/RAR α were located at enhancer regions (Figure 3A). Surprisingly, we also found that PML/RAR α preferentially co-occupied enhancers with higher H3K27ac signals (Figure 3B; supplemental Figure 5), which met the criteria of super-enhancers.¹² We further assessed the binding tendency of PML/RAR α on 2 categories of enhancers, super-enhancers and typical enhancers, and found that PML/RAR α was over fourfold more likely to co-occupy super-enhancers than typical enhancers (80.6% vs 19.0%; Figure 3C; supplemental Table 9). Similar results (threefold, 60.6% vs 21.5%) were observed in primary APL blasts (Figure 3C; supplemental Table 10). At the gene level, we identified a total of 303 super-enhancer-associated PML/RAR α -regulated targets (SEPRTs; supplemental Table 11). To illustrate the functional importance of SEPRTs in APL, we used a CRISPR-Cas9 screening data set in NB4 cells³⁸ to perform GSEA, showing that SEPRTs tended to be enriched among genes essential for cell growth (Figure 3D), such as GF11, IKZF1, and JUNB.

ATRA and ATO exert synergistic effects on controlling SEPRTs in APL cells

Next, we explored how SEPRTs responded to ATRA and ATO, 2 widely used drugs in APL therapy. We performed RNA-seq in NB4 cells treated with ATRA or ATO in a time series, from which differentially expressed genes were identified. Using self-organizing map-based gene clustering and visualization, we identified 3 gene clusters (C1-C3; Figure 4A; supplemental Table 12) and found that ATRA and ATO shared some similar regulatory effects (genes in C1 downregulated by both ATRA and ATO) but also exerted different impacts; genes in C2 were only downregulated by ATO, as early as 6 hours after treatment (such as *GF11* and *ETS1*), while genes in C3 only upregulated by ATRA, with trivial effects upon ATO treatment.

Functional enrichment analysis of gene clusters (Figure 4B; supplemental Table 13) showed that genes in C1 are functionally involved in the apoptotic process and regulation of cell death, such as *RUNX2* and *CTSH*. Genes in C2 are of functional relevance to endocytosis, such as *ARRB1* and *MAPKAPK3*. Genes in C3 are functionally essential for myeloid leukocyte activation (eg,

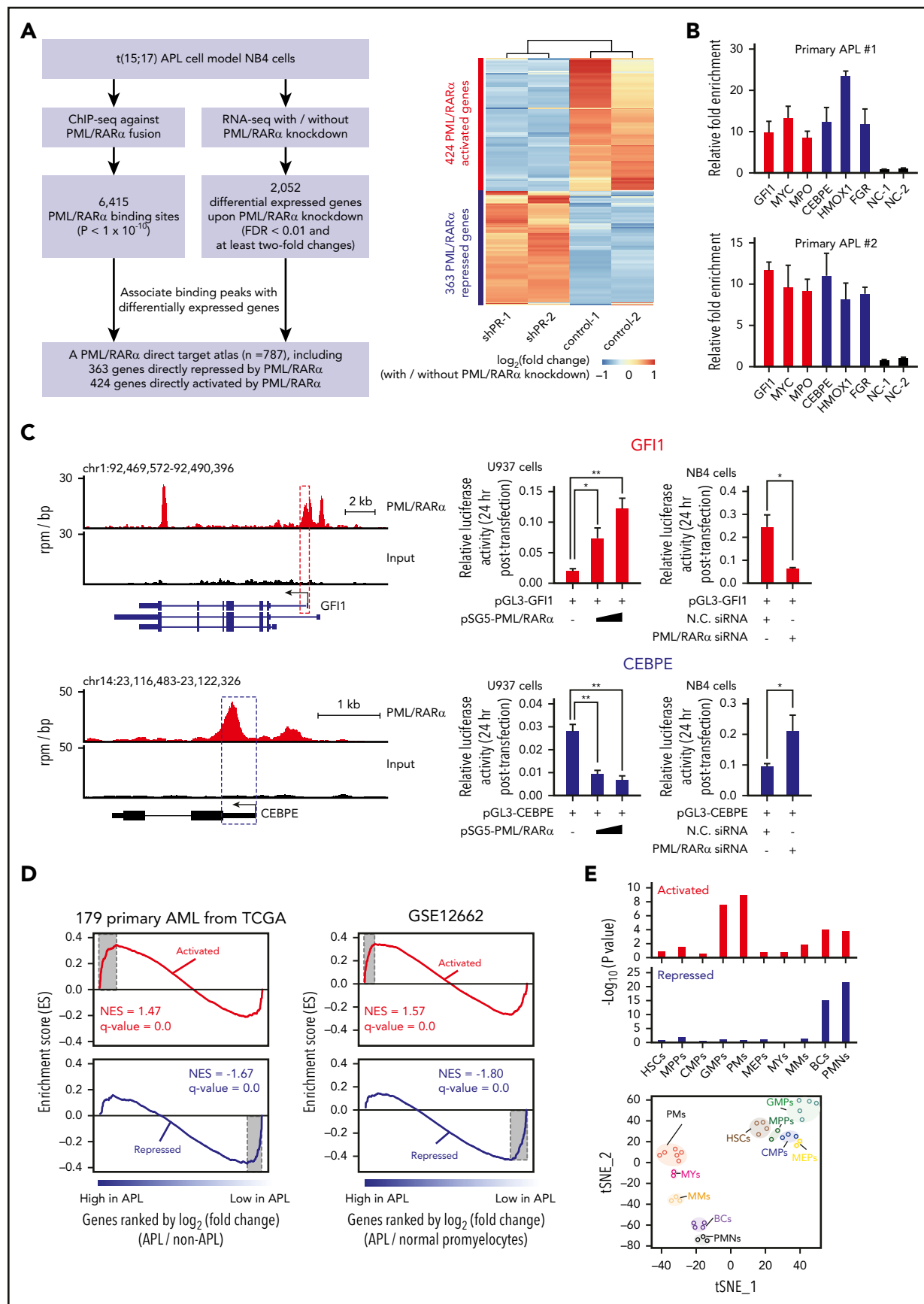


Figure 1. PML/RAR α exerts both repressive and activating functions through direct binding. (A) Genome-wide identification of PML/RAR α direct target genes from integrative assays of ChIP-seq and RNA-seq. Schematic illustration of the experimental design, including the criteria used for analysis (left). Heatmap showing the expression change of the identified direct target genes upon PML/RAR α knockdown (right). Two classes of target genes were categorized: PML/RAR α -repressed targets (in blue) and

SPI1, SUCNR1, and PIK3CD), suggesting that these genes might contribute to ATRA-induced differentiation. Also, genes associated with coagulation (eg, PLEK and PTPN6) were enriched in C3, suggesting that the effect of ATRA in alleviating coagulation may be attributed to the regulation of SEPRs as well. We also explored evidence supporting therapeutic potential by identifying the crosstalk between pathways from our time-course expression data and pathway interaction data (see supplemental Methods). This identified synergistically regulated genes (CTSH and PRKCD) and targets (PIK3CD and RRM2) of approved drugs in other diseases, supporting repurposing opportunities and potential efficacy (Figure 4C). Together, these results indicated that ATO and ATRA can act through SEPRs, likely explaining the combination use in APL therapy.

PML/RAR α -activated GFI1 is necessary for the maintenance of APL

The functional significance of PML/RAR α -mediated repression in APL has been intensively investigated; however, little attention is paid to PML/RAR α -mediated activation. As an exemplar, we performed more detailed functional experiments on *GFI1*, the gene encoding a TF known to be involved in the development of hematopoietic stem cells³⁹ and lymphocytes.²² We found that *GFI1* knockdown induced a partial granulocytic differentiation and apoptosis, promoted the G0/G1 phase arrest, and reduced the colony-forming abilities of NB4 cells (Figure 5A-E; supplemental Figure 6A). This finding was also verified in primary APL blasts (Figure 5F; supplemental Figure 6B).

Moreover, we determined the *in vivo* role of Gfi1 using a transplantable APL mouse model, which closely mimics human APL with similar biological characteristics.⁴⁰ PML/RAR α -positive leukemic cells from APL transplantable mice were transduced with shRNAs targeting *Gfi1* and then transplanted into the recipient FVB/NJ mice (Figure 5G; supplemental Figure 7). As shown in Figure 5H-K, transplantable blasts with *Gfi1* knockdown could not efficiently develop leukemia, as characterized by no obvious tumor burden observed in the recipients. The results suggested that GFI1 is necessary for the maintenance of APL.

PML/RAR α transactivates *GFI1* through chromatin conformation at the super-enhancer region

Since PML/RAR α can form as heterodimers or oligomers through the RBCC domain,⁴¹ it is tempting to speculate that PML/RAR α might transactivate *GFI1* through chromatin conformation at the super-enhancer region. We first exploited 3C-PCR⁴² to examine

the chromatin structure at the super-enhancer region of *GFI1* in NB4 cells (Figure 6A). There existed 3 PML/RAR α -bound *cis* elements at the *GFI1* locus: the promoter (peak 1), the intronic enhancer (peak 2) and the distal enhancer (peak 3). The loop linking the intronic enhancer (peak 2) to the other 2 *cis* elements showed the strongest interaction, consistent with the highest PML/RAR α binding on this site observed in ChIP-seq (top-left panel in Figure 6A).

Using a PML/RAR α -inducible cell line (supplemental Figure 8A), we found that the interaction between the intronic enhancer and the promoter became significantly stronger upon PML/RAR α induction (Figure 6B), confirming the importance of PML/RAR α for super-enhancer formation, mainly through binding on the intronic enhancer. To test the outcome of PML/RAR α -mediated chromatin conformation, we generated a construct containing the intronic enhancer cloned upstream of the *GFI1* promoter and found that this construct resulted in a 2.5-fold increase in luciferase activity compared with the promoter construct lacking the enhancer activity (Figure 6C). We further used PML/RAR α -F158E (with the mutation in the RBCC domain impairing oligomerization⁴³) to determine the contribution of PML/RAR α oligomerization. We found that chromatin conformation at the *GFI1* locus was barely seen and the associated transcriptional activation was significantly reduced in mutant cells (Figure 6D-E; supplemental Figure 8B), indicating that PML/RAR α , likely oligomerized, transactivated *GFI1* through chromatin conformation.

Next, we determined the effect of PML/RAR α binding on super-enhancer regulation in APL development using CRISPR-dCas9-mediated technology,⁴⁴ which is capable of disrupting PML/RAR α binding and eliciting a silencing event on the targeted region. We designed the single guide RNA (sgRNA) targeting the PML/RAR α -enriched loci within the intronic enhancer region of *GFI1* (sg-*GFI1e*) and transduced it into dCas9-KRAB stably expressing NB4 cells (Figure 6F). As shown in Figure 6G, the perturbation of PML/RAR α binding led to the reduced *GFI1* expression, demonstrating that *GFI1* activation depended on PML/RAR α binding to this enhancer. Also, these sgRNA-transduced dCas9-KRAB-expressing cells were able to differentiate into terminal granulocytes (Figure 6G; supplemental Figure 9). When these cells transplanted into NOD/SCID mice, we found that leukemia could not be efficiently developed (Figure 6H). Together, the *in vitro* and *in vivo* evidence demonstrated that PML/RAR α -mediated activation on the *GFI1* super-enhancer was required for the development of APL.

Figure 1 (continued) PML/RAR α -activated targets (in red). The maximum distance of 50 kb was used to associate ChIP-seq peaks with the nearest differentially expressed genes identified by RNA-seq. (B) Validation of PML/RAR α targets in primary APL samples. ChIP-qPCR was performed on primary blasts from 2 APL patients using the antibody against the fusion site of PML/RAR α . Negative controls include 2 irrelevant genomic regions with no PML/RAR α binding signals (NC-1 and NC-2). Validation of PML/RAR α targets in NB4 cells can be found in supplemental Figure 3. (C) PML/RAR α effects on transcriptional activities of the directly repressed gene *CEBPE* (bottom right) or the directly activated gene *GFI1* (top right). The left panel shows the genome browser tracks of PML/RAR α binding, with the regions cloned in the luciferase constructs highlighted in dotted box. The luciferase reporter plasmid of each detected region was cotransfected with the PML/RAR α -expressing plasmid in U937 cells or small interfering RNA (siRNA) targeting the fusion site of PML/RAR α in NB4 cells. Luciferase activity was detected at 24 hours after transfection. N.C. siRNA, nonspecific siRNA control. Data represent the mean of 3 replicates \pm standard deviation (SD). Statistical significance was determined using the unpaired, 2-tailed Student t test. * $P < .01$, ** $P < .001$. chr, chromosome. (D) GSEA in terms of differentially expressed genes identified comparing blasts from 16 APL patients vs 163 non-APL AML patients (left panel) and comparing APL patients vs normal promyelocytes (right panel). NES, normalized enrichment score. (E) Enrichment analysis of PML/RAR α -activated and repressed targets using the gene sets signifying genes specifically expressed in each of 10 stages of myeloid differentiation. t-Distributed stochastic neighbor embedding (t-SNE) plots showing the 10 stages of myeloid differentiation constructed using the transcriptome data of sorted hematopoietic stem cells, myeloid progenitors, and their mature progeny (bottom panel). The statistical significance of the enrichment was determined by the hypergeometric test (top panel). BCs, band cells; CMPs, common myeloid progenitors; GMPs, granulocyte/monocyte progenitors; HSCs, hematopoietic stem cells; MEPs, megakaryocyte/erythroid progenitors; MMs, metamyelocytes; MPPs, multipotential progenitors; MYs, myelocytes; PMs, promyelocytes; PMNs, polymorphonuclear cells. Red bars represent PML/RAR α -activated targets, and blue bars represent PML/RAR α -repressed targets.

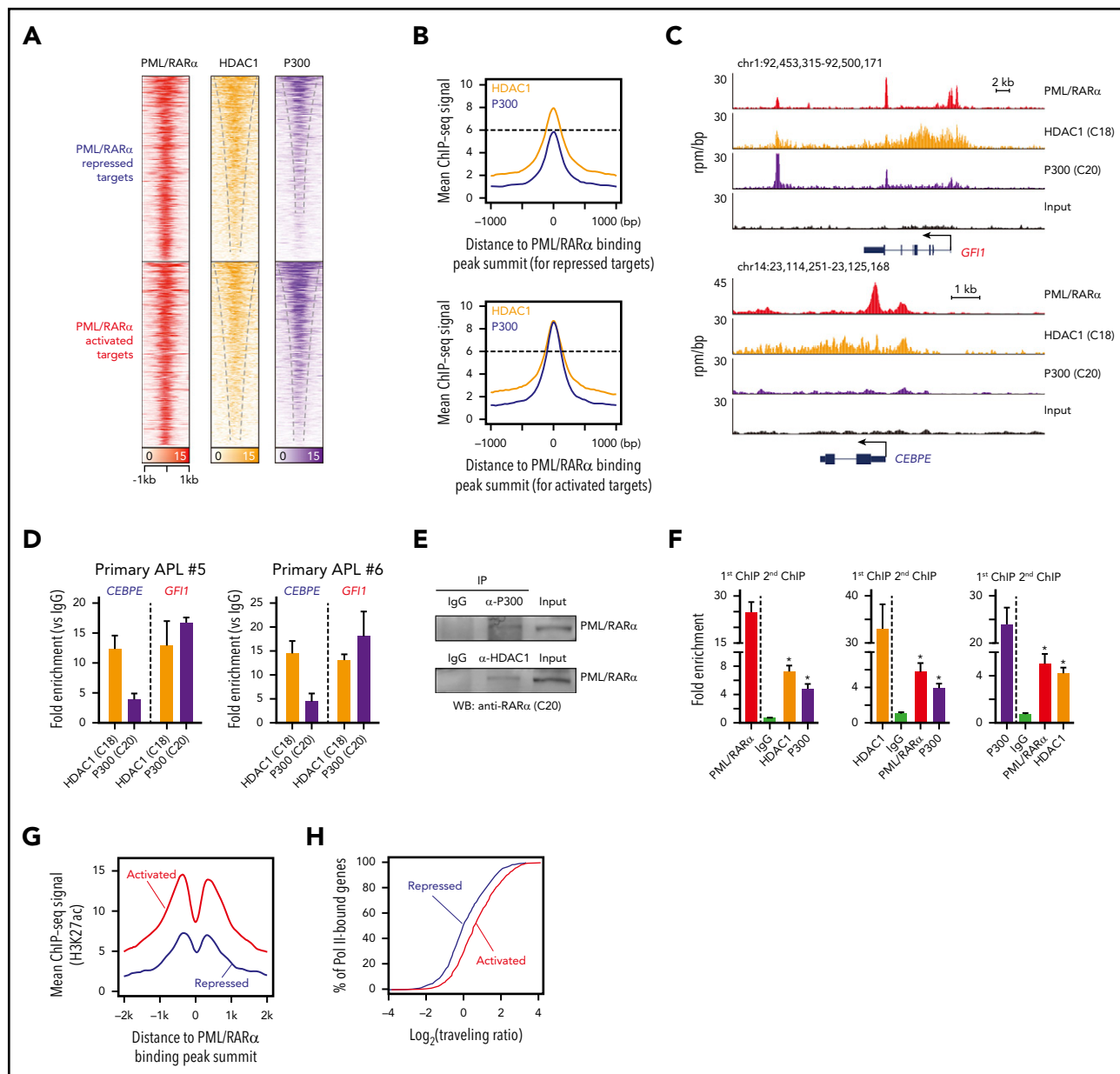


Figure 2. Repressive and activating functions of PML/RARα are attributed to distinct cobinding patterns with HDAC1 and P300. (A) Heatmaps of ChIP-seq data showing cobinding of HDAC1 and P300 at the PML/RARα binding sites, displayed separately for PML/RARα-repressed targets (the top half) and -activated targets (the bottom half). (B) Abundant enrichment of both HDAC1 and P300 on PML/RARα-activated targets vs abundant HDAC1 with moderate/minor P300 on PML/RARα-repressed targets, illustrated using aggregate plots of ChIP-seq signals of HDAC1 and P300 centered on the PML/RARα binding peak summit. (C) Genome browser tracks showing the binding patterns of PML/RARα, HDAC1, and P300 on the representative repressed gene (*CEBPE*) and activated gene (*GFI1*). (D) ChIP-qPCR validation of distinct HDAC1 and P300 cobinding patterns on PML/RARα-repressed and activated targets in blast cells from 2 primary APL patients. (E) The physical interaction of both HDAC1 and P300 with PML/RARα. Endogenous coimmunoprecipitation (co-IP) experiments were performed in NB4 cells using antibodies against HDAC1 and P300, respectively. The protein level of PML/RARα was detected by western blotting with anti-RARα antibody (C20). IgG, immunoglobulin G; WB, western blot. (F) ChIP-re-ChIP showing co-occupancy of PML/RARα, HDAC1, and P300 on chromatin. ChIP products immunoprecipitated by each of the 3 antibodies were subjected to re-ChIP using the other 2 antibodies or normal immunoglobulin G. Data represent the mean of 3 replicates ± SD. **P* < .01. (G) Aggregate plots of H3K27ac ChIP-seq signals centered on the PML/RARα peak summit. Red, PML/RARα-activated targets; blue, PML/RARα-repressed targets. (H) Enrichment of RNA Pol II at genes activated and repressed by PML/RARα. The activity of Pol II was determined by the Pol II traveling ratio, which was calculated by the relative amount of Pol II binding at the gene body vs near the promoter. Red, PML/RARα-activated targets; blue, PML/RARα-repressed targets. The 2-sample Kolmogorov-Smirnov test was used to compare distributions (*P* < .001).

Analysis of GFI1 targets and evidence supporting coregulation with PML/RARα

We reasoned that analyzing GFI1 targets particularly comparing with PML/RARα targets could allow us to deduce the interplay between GFI1 and PML/RARα in APL cells. We first performed ChIP-seq of GFI1 in NB4 cells and identified 1603 binding sites

shared by both PML/RARα and GFI1 (Figure 7A; supplemental Table 14). Interestingly, motif analysis revealed that the most significant motifs were those for myeloid TFs (the top 3 included CEBPA, ETS, and RUNX1) (Figure 7B), whereas for all GFI1 ChIP regions, the most significant was as expected the canonical GFI1 motif (supplemental Figure 10A). This observation was supported

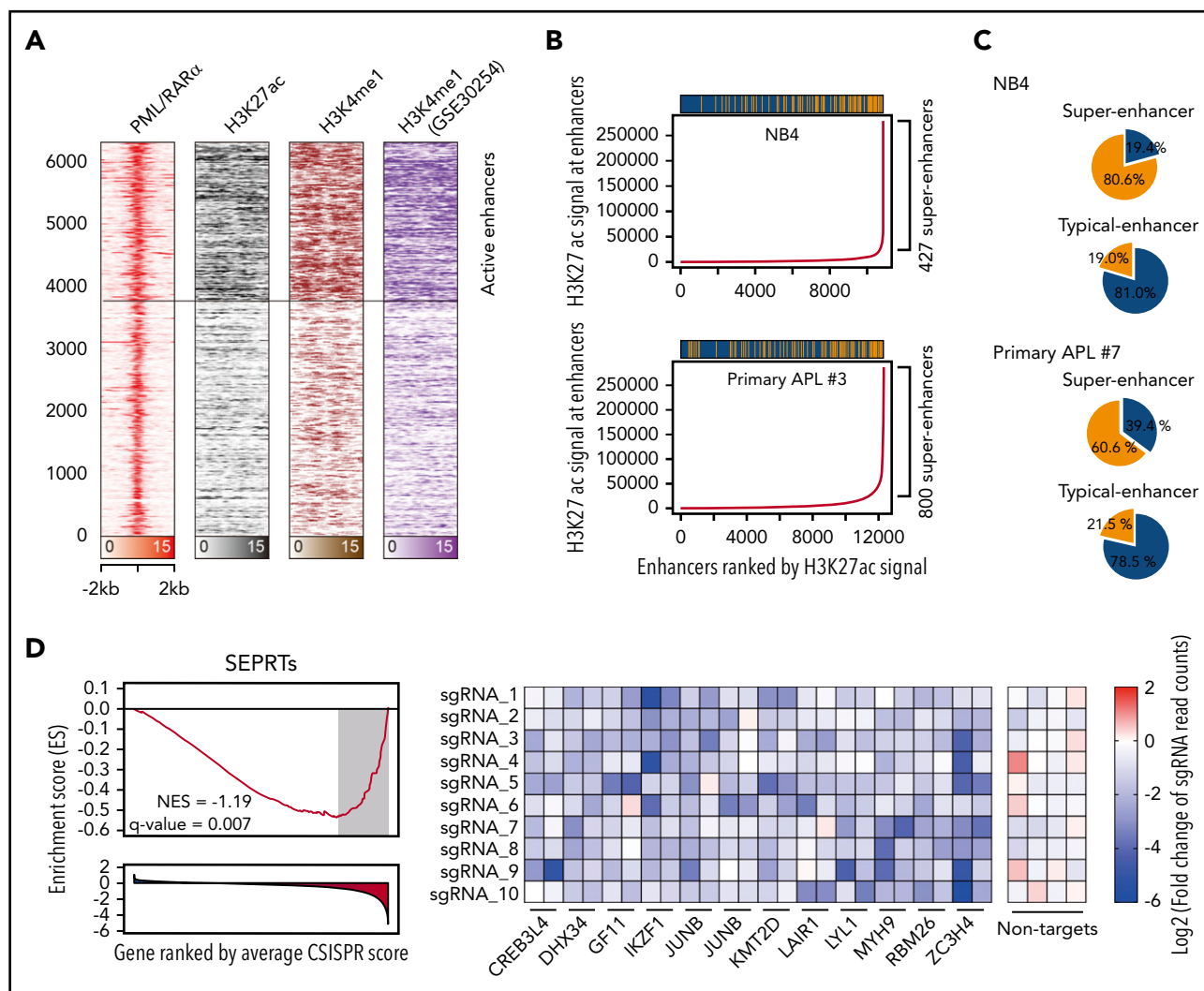


Figure 3. PML/RAR α coexists within the super-enhancer regions to regulate APL-specific genes. (A) Heatmap showing abundant PML/RAR α , H3K27ac, and H3K4me1 occupancy on PML/RAR α binding sites, with those indicative of active enhancers highlighted. (B) PML/RAR α tended to bind at enhancers with higher H3K27ac signals in APL cells, including NB4 (upper panel) and primary blasts (lower panel). Enhancers were ranked by the H3K27ac signal. Super-enhancers were defined using the ROSE methods (detailed in supplemental Methods). The bar above shows the distribution of PML/RAR α binding among enhancers, in which the yellow represents the peak with PML/RAR α binding and the blue for the peak without PML/RAR α binding. (C) PML/RAR α preferentially bound super-enhancers three- to fourfold more likely than typical enhancers in APL cells, including NB4 (upper panel) and primary blasts (lower panel). Pie plots show the percentages of PML/RAR α binding within the super-enhancer regions and typical enhancer regions. (D) SEPRTs essential for the survival of APL cells, supported by CRISPR-Cas9 screening data in NB4 cells. The left panel shows GSEA using the SEPRTs and CRISPR score. The CRISPR score was used to rank 18 661 genes in the CRISPR-Cas9 screen applied to NB4 cells. The right panel shows normalized read counts of sgRNA in NB4 cells transfected with the Cas9-CRISPR/sgRNA library before and after population doublings.

by published ChIP-seq data on RUNX1⁴⁵ and the ETS family member FLI1⁴⁶ (Figure 7C; supplemental Figure 10B). This suggested that PML/RAR α and GFI1 might be assembled with a number of myeloid TFs to coregulate the corresponding target genes, consistent with the notion that multiple TFs coordinately regulate lineage-specific gene expression.⁴⁷ Functional enrichment analysis supported that coregulated target genes were indeed of functional relevance to myeloid differentiation and myeloid-related activities (Figure 7D).

Next, we conducted RNA-seq experiments in NB4 cells with and without GFI1 knockdown. GSEA showed that coregulated genes were significantly enriched within GFI1-repressed genes (Figure 7E), consistent with the previously identified role of GFI1 as a transcriptional repressor.⁴⁸ Interestingly, coregulated genes were also significantly enriched within GFI1-activated genes

(Figure 7E). When inspecting genes significantly regulated upon PML/RAR α knockdown, we found that PML/RAR α also activated these GFI1-activated genes, such as CXCR4 and MPO (supplemental Figure 10C). This motivated us to further explore the role of GFI1 on PML/RAR α -mediated transactivation on these coregulated genes. We found that the binding of PML/RAR α on coactivated genes was dramatically decreased in NB4 cells after GFI1 knockdown (Figure 7F). Together, the results suggested that GFI1 might coordinate with the activating function of PML/RAR α on these cobound and coactivated genes.

Discussion

Genome-wide identification of direct targets, particularly a larger number of activated targets, challenges the longstanding view of PML/RAR α being a transcriptional repressor. This direct

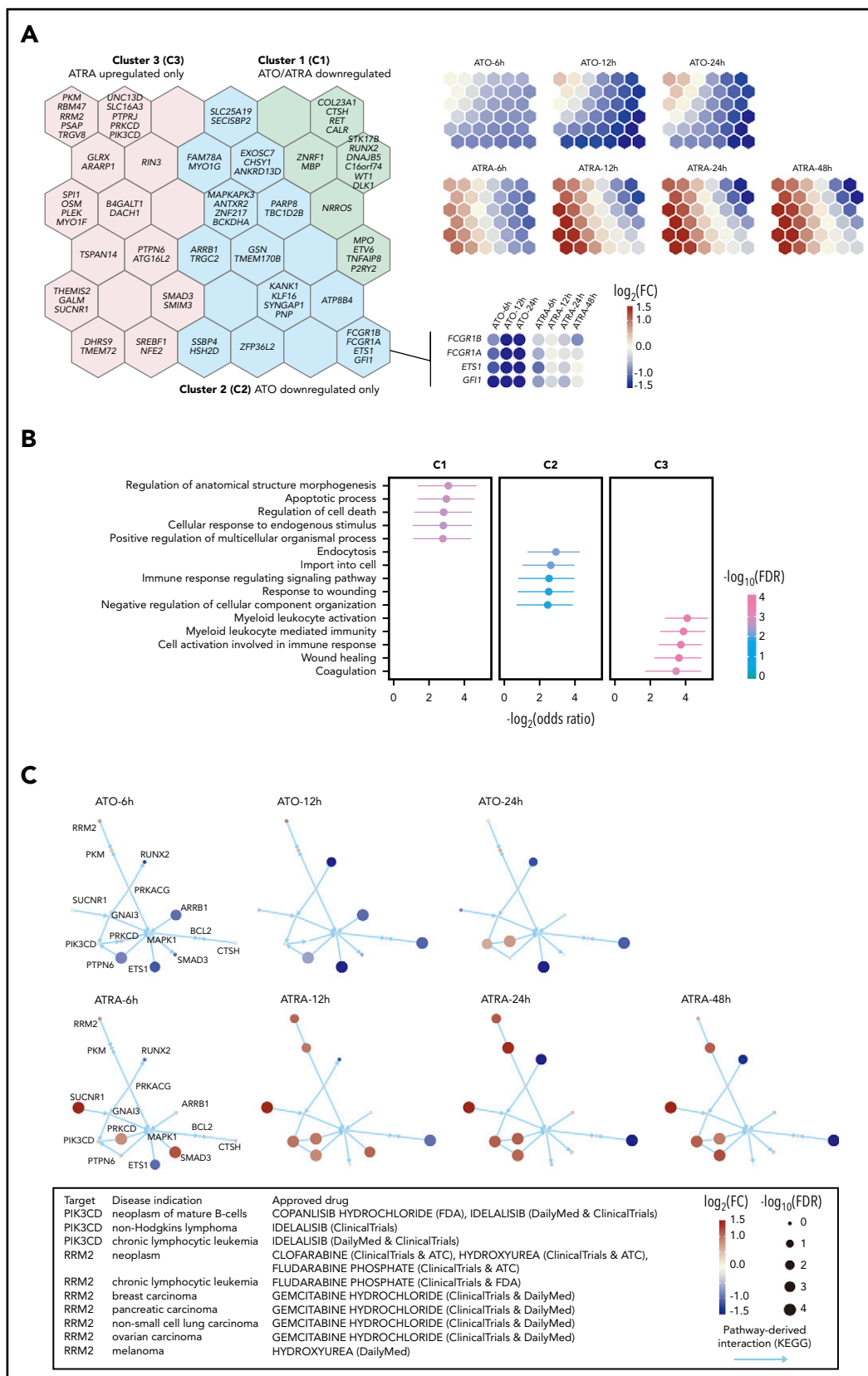


Figure 4. ATRA and ATO exert synergistic effects on controlling SEPRTs in APL cells. (A) Clustering of SEPRTs after ATRA or ATO treatment using self-organizing map. The left panel shows 3 gene clusters color-coded on the map, with per-hexagon genes labeled (for example, genes in the insert with heatmap showing expression pattern). The right panel shows that each presentation indicates treatment- and time-specific changes, in which upregulated (red), downregulated (blue), and no changed (light yellow) genes are well separated. FC, fold change. (B) Functional enrichments in gene clusters. Gene Ontology Biological Process terms were used for enrichment analysis based on the Fisher exact test (1 sided), with odds ratios and 95% confidence interval calculated. FDR, false discovery rate. (C) Pathway crosstalk identified from integrative analysis of time course expression data and known pathway interaction data. The crosstalk illustrated in the same layout but nodes (genes) colored and sized in a treatment- and time-specific manner. Current approved drug therapeutics for crosstalk genes based on the ChEMBL database. ATC, anatomical therapeutic chemical; FDA, US Food and Drug Administration.

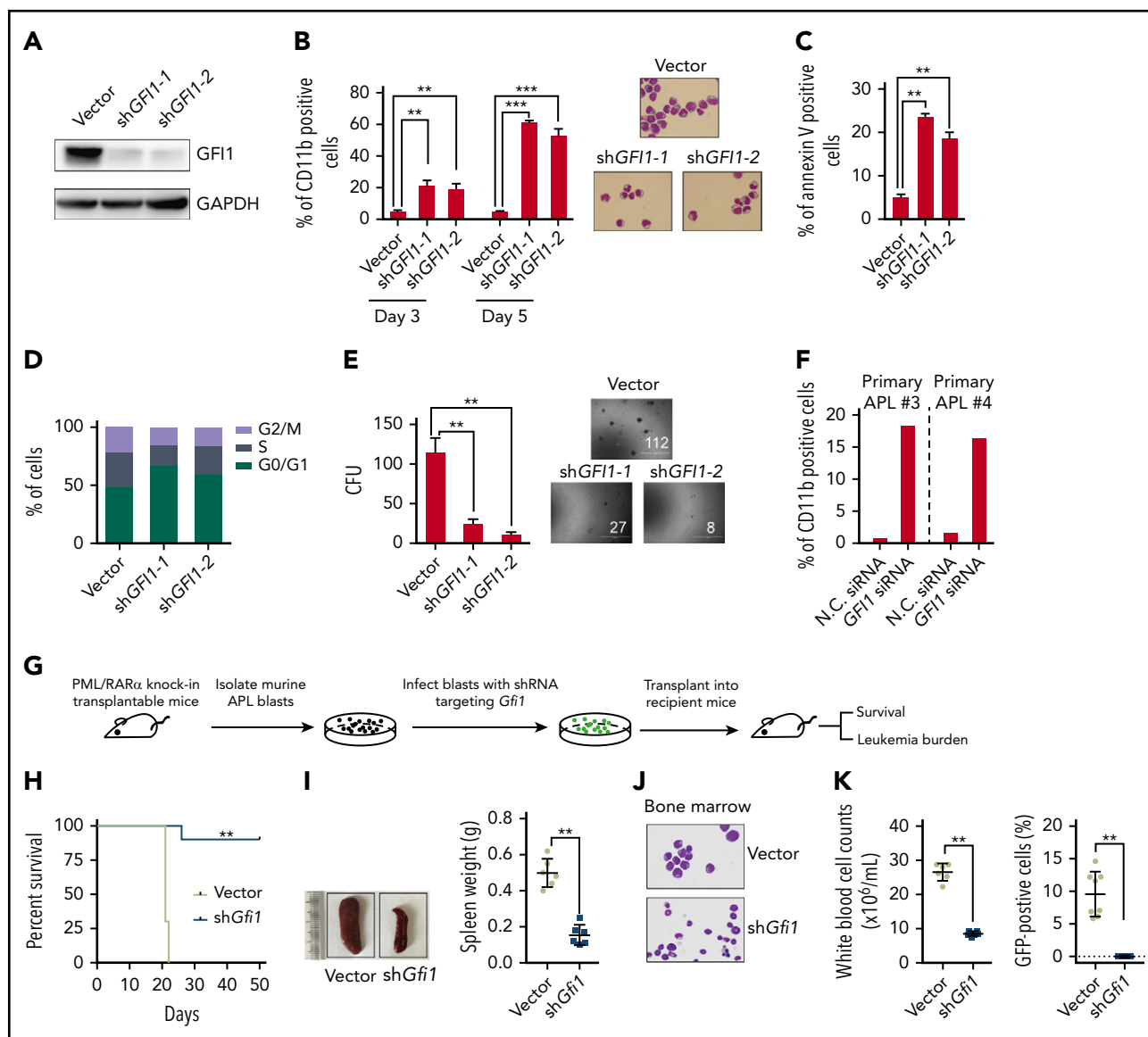


Figure 5. PML/RAR α -activated GFI1 is necessary for the maintenance of APL. (A-E) Detailed shRNA-mediated loss-of-function analyses on PML/RAR α -activated GFI1. Western blot was performed to validate the knockdown efficiency of shRNAs targeting GFI1 (A). Knockdown of GFI1 induced partial differentiation (B) and apoptosis (C), promoted the G₀/G₁ phase arrest (D), and decreased the colony-forming capacity (E). The expression of the cell surface differentiation marker CD11b in shGFI1 positively transfected cells was determined by flow cytometry and the morphology was detected by Wright-Giemsa staining. Apoptosis was detected in NB4 cells after transfection of shRNA constructs for 4 days and determined by Annexin V-APC staining. Data represent the mean of 3 replicates \pm SD. ** P < .001, *** P < .0001. (F) GFI1 function was verified in primary APL blast cells. GFI1 siRNAs or negative control (N.C.) were transfected into blast cells isolated from 2 primary APL patients. (G) The schematic diagram of the in vivo experiment. Murine APL blasts isolated from transplatable APL mice were transduced with the shRNA targeting *Gfi1*, and then the shRNA-positive cells with ZsGreen1 expression were sorted and transplanted into the recipient FVB/NJ mice. The shRNA empty vector was used as the control. (H) Altered disease onset of APL after *Gfi1* knockdown. PML/RAR α -positive leukemia cells separated from APL transplatable mice (n = 6) were transduced with shRNA targeting *Gfi1* or vector and then transplanted into recipient mice. The statistical significance was calculated by the log-rank (Mantel-Cox) test. ** P < .001. (I) Knockdown of *Gfi1* in murine APL cells resulted in no obvious splenomegaly in APL transplatable mice. Left panels show the representative images of the spleen. ** P < .001. (J) Murine APL blasts were hardly seen in bone marrow of mice upon *Gfi1* knockdown, as shown by representative Wright-Giemsa staining of bone marrow smears. (K) The tumor burden in the peripheral blood of mice transplanted with PML/RAR α -positive cells with GFI1 knockdown, as compared with those transplanted with cells without GFI1 knockdown. The left panel shows the total white blood cell counts, and the percentage of GFP-positive abnormal promyelocytes is shown in the right panel. ** P < .001.

target atlas provides a more complete picture of PML/RAR α -driven oncogenesis: PML/RAR α represses genes responsible for hematopoiesis and activates super-enhancer genes responsible for APL-specific characteristics.

We redefine the activation role of PML/RAR α in APL. Particularly, we provide rich evidence supporting the functional importance of PML/RAR α -activated target gene *GFI1* in APL. We demonstrate

that *GFI1* can coordinate with PML/RAR α to maintain APL and that PML/RAR α -induced differentiation block can be relieved upon *GFI1* knockdown. Our findings differ from the previous reports that loss or reduced level of *GFI1* impedes generation of granulocytes^{49,50} but rather support that GFI1 has context-dependent roles in leukemogenesis (in APL depending on PML/RAR α). Of note, by reanalyzing the expression data from APL blasts and normal promyelocytes,²⁹ we reveal that GFI1 is

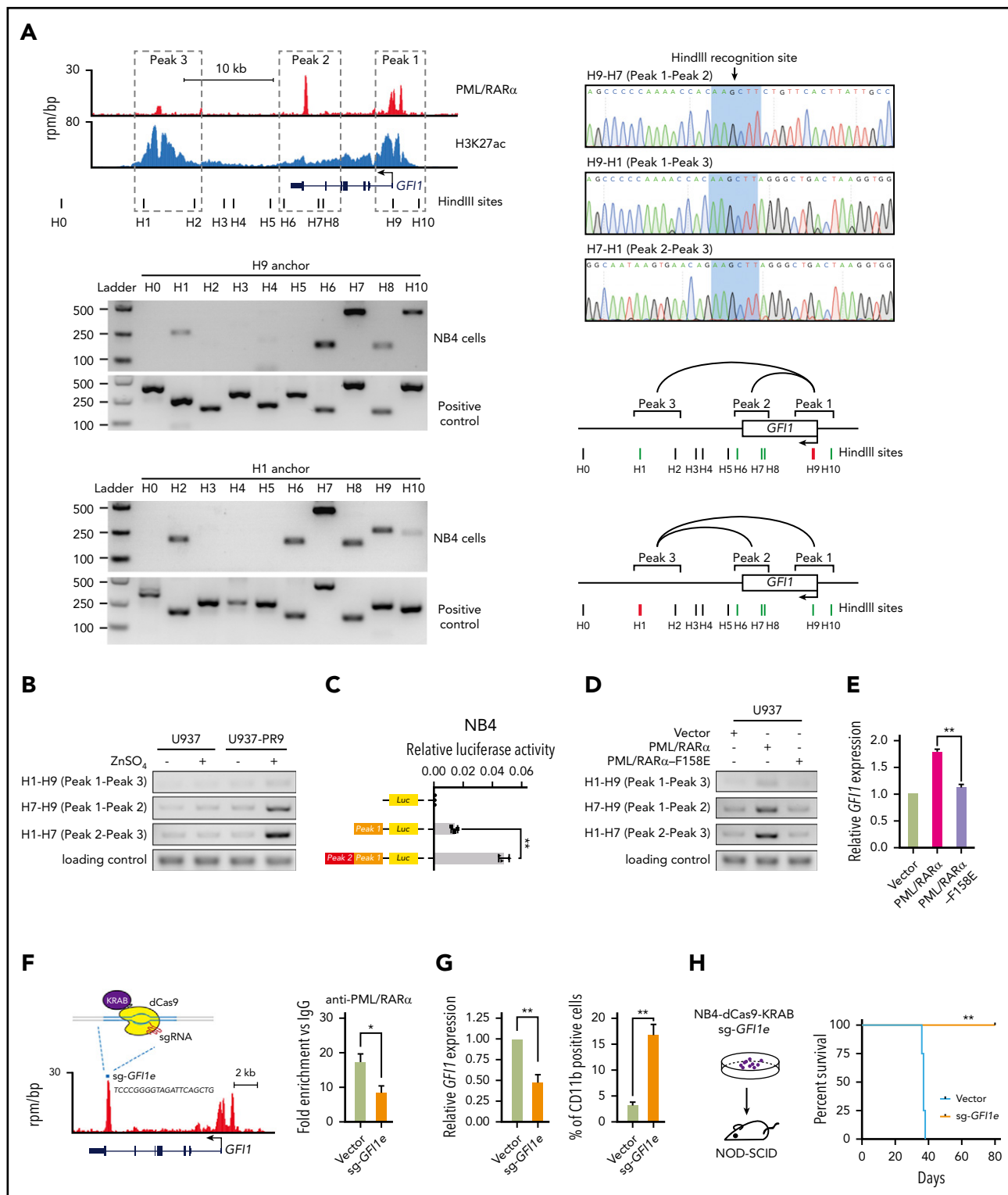


Figure 6. PML/RAR α transactivates GFI1 through chromatin conformation at the super-enhancer. (A) Chromatin conformation of the PML/RAR α -bound super-enhancer region on the GFI1 locus in NB4 cells. Genomic browser tracks (top-left panel) show 3 PML/RAR α binding peaks corresponding to the promoter (assigned by peak 1), the intronic enhancer (peak 2), and the distal enhancer (peak 3) at the super-enhancer region of GFI1, with black bars indicating the cutting sites of HindIII. The interactions among 3 peaks were determined by the 3C-PCR experiments, with results shown in bottom-left panels and the schematic illustration in bottom-right panels. The anchor primers (ie, H1 and H9) are indicated by red bars. The positive and negative interactions between the anchor primer and the paired 3C primer are indicated by green and black bars, respectively. The curve line represents the interaction between the indicated peaks. Also shown are the sequencing results of the cut and religated sequences of the 3C-PCR products (top-right panel), confirming the interactions between peak 1 (H9) and peak 2 (H7), peak 2 (H7) and peak 3 (H1), and peak 1 (H9) and peak 3 (H1). (B) PML/RAR α determined the interaction between the intronic enhancer and the promoter of GFI1. The interactions between each pair of 3 cis elements were determined by 3C-PCR with and without PML/RAR α protein induced in the PML/RAR α -inducible cell line (U937-PR9). (C) PML/RAR α -mediated chromatin conformation resulted in the activation of GFI1. The *trans* activity was determined by the dual luciferase reporter assays in NB4 cells. Peak 1 represents the promoter and peak 2 represents the intronic enhancer as illustrated in Figure 6A. ** $P < .001$. (D-E) PML/RAR α

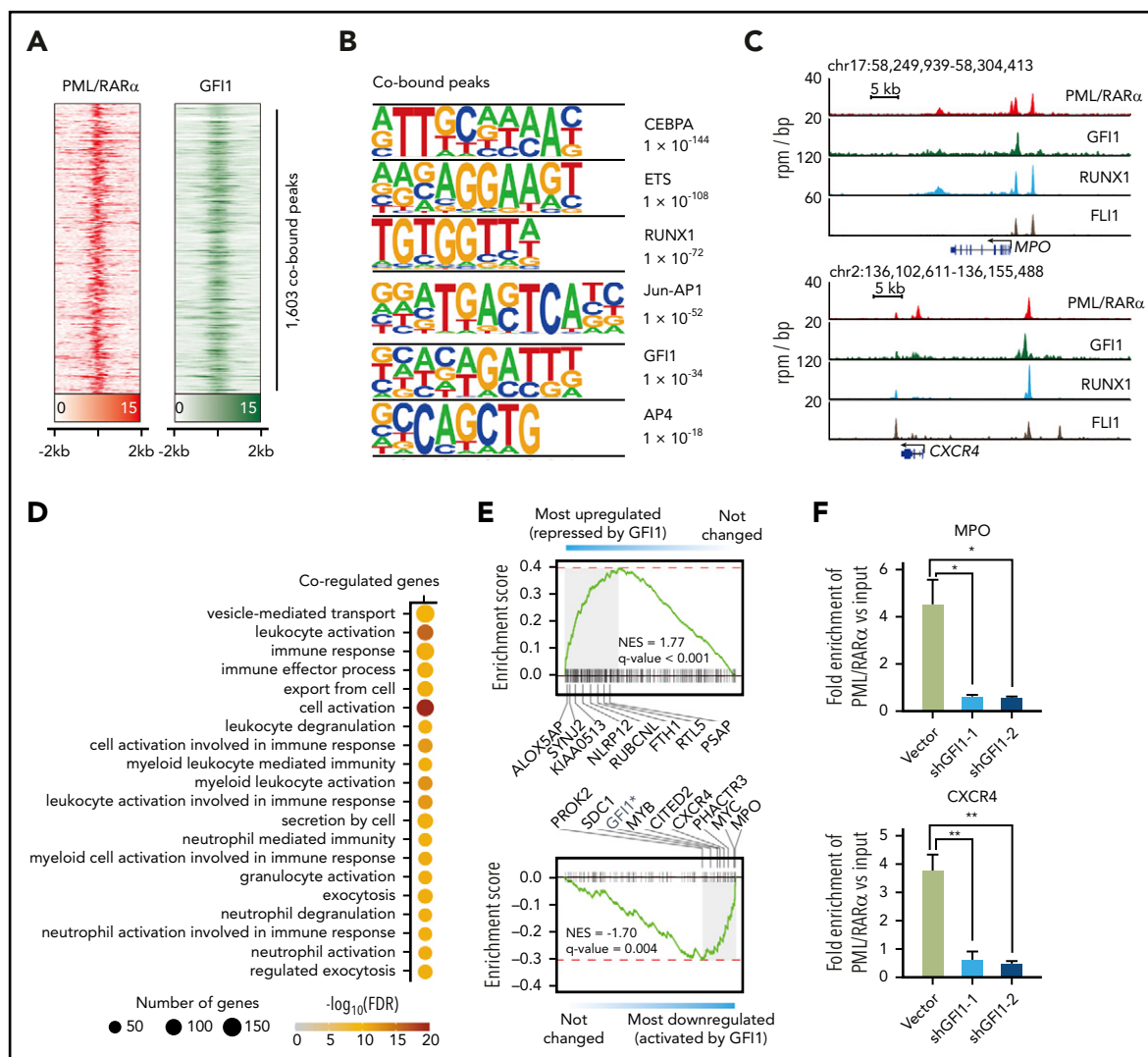


Figure 7. Analysis of GFI1 targets and their association with PML/RARα targets. (A) Heatmap showing the ChIP-seq signals of PML/RARα and GFI1 centering on the binding summit of PML/RARα and GFI1 cobound peaks. (B) Motif analysis of peaks cobound by PML/RARα and GFI1. Top 6 enriched motifs were shown. (C) Genome-browser tracks showing the binding of PML/RARα, GFI1, RUNX1, and FLI1 on the regulatory regions of CXCR4 and MPO in NB4 cells. (D) Gene Ontology enrichment analysis showing Biological Process terms enriched on PML/RARα and GFI1 coregulated genes. (E) GSEA of PML/RARα and GFI1 coregulated genes in terms of differential genes upon shRNA-mediated knockdown of GFI1 (indicated by graded bars). Also labeled are representative genes found at the leading edge. NES, normalized enrichment score. The asterisk indicates that GFI1 downregulation was due to knockdown using shGFI1. (F) Knockdown GFI1 decreased PML/RARα binding on chromatin of GFI1 and PML/RARα cobound and coactivated genes MPO and CXCR4. ChIP-qPCR of PML/RARα binding was performed in NB4 cells with or without GFI1 knockdown. The fold enrichment of ChIPed samples vs input was plotted in the y-axis. * $P < .01$, ** $P < .001$.

maintained at the high expression level in both samples, though PML/RARα-activated targets as a whole tend to be malignant related (APL vs normal promyelocytes) and APL specific (APL vs non-APL AML) (Figure 1D; supplemental

Figure 4). It implicates that some of activated targets, such as GFI1, are dedicated to transcriptional programs needed to maintain the promyelocytic stage for APL (maintained consistently) or normal promyelocytes (transiently). We have

Figure 6 (continued) oligomerization was required for the chromatin conformation regulation at the GFI1 locus and the subsequent activation of GFI1. The interactions between peaks at the GFI1 locus were examined by 3C-PCR (D) and relative expression of GFI1 detected by reverse transcription (RT)-qPCR (E) in U937 cells transfected with wild-type PML/RARα or PML/RARα mutant (PML/RARα-F158E) for which oligomerization was impaired due to the mutation in the RBCC domain. ** $P < .001$. (F) Schematic illustration of the CRISPR-dCas9-KRAB-mediated interruption of PML/RARα binding and regulation on the super-enhancer of GFI1. sg-GFI1e, targeting the PML/RARα-enriched loci on the GFI1 intronic enhancer (peak 2), was transduced into dCas9-stably expressing NB4 cells. The right panel shows the decrease of PML/RARα binding on the super-enhancer of GFI1 determined by ChIP-qPCR. * $P < .01$. (G) Direct interruption of PML/RARα binding and regulation on the enhancer region of GFI1 decreased GFI1 expression (left panel) and subsequently induced granulocytic differentiation of NB4 cells (right panel). Relative expression of GFI1 was detected by quantitative reverse transcription qPCR. The percentage of CD11b-positive cells was detected 3 days after sgRNA transduction and determined by flow cytometry. Data represent the mean of 3 replicates \pm SD. ** $P < .001$. (H) Direct interruption of PML/RARα binding and regulation on the enhancer region of GFI1 interfered with the occurrence of APL in vivo. The sgRNA-transduced dCas9-expressing NB4 cells targeting GFI1 intronic enhancer were injected into NOD/SCID mice. The Kaplan-Meier analysis was used to estimate the survival of mice. Statistical significance was calculated by the log-rank (Mantel-Cox) test. ** $P < .001$.

observed very little overlap of our direct targets with differentially expressed genes reported from the PML/RAR α -transgenic preleukemic mice study, in keeping with previous studies.²³ These observations call for future studies to clarify the exact function of GFI1 in the initiation and development of APL as well as promyelocyte development.

Equally interesting is that ATO can significantly reverse the activation of GFI1, whereas ATRA has minimal effect (Figure 4A). This seems to be consistent with (1) our observation that ATO, capable of rapidly degrading PML/RAR α ,^{41,51} can dramatically reduce PML/RAR α , HDAC1, and P300 binding and also interrupt the chromatin conformation at the super-enhancer region of *GFI1* (supplemental Figure 11); and (2) the fact that ATRA can release PML/RAR α binding only at the late stage of differentiation by activating the ubiquitin proteasome system.^{52,53}

How PML/RAR α activates gene expression has been largely undocumented. The prevailing view is that before ATRA treatment, PML/RAR α recruits only HDAC1, which is then replaced with P300 after ATRA treatment.³ Our data challenges this view. We show that in the absence of retinoic acid, PML/RAR α can interact with abundant P300 and HDAC1 on chromatin (though not necessarily colocalized on the same site of chromatin) to activate gene expression, likely in a ligand-independent manner. Although fetal bovine serum used for cell culture might contain traces of retinoids, the contribution of ATRA might be below the physiological level (supplemental Figure 12). The further addition of the physiological concentration (1 nM) of ATRA has trivial impact on such activation (supplemental Figure 12), supporting ligand independency of PML/RAR α -mediated activation. There is considerable evidence to support our findings. Firstly, histone deacetylases (HDACs) may help prevent inappropriate reinitiation of transcription on regulatory regions simultaneously bound by histone acetyltransferases and HDACs.⁵⁴ Secondly, genome-wide profiling of chromatin-modifying enzymes has indicated that histone acetyltransferases and HDACs can be colocalized on highly active transcribed regions.^{2,55} Thirdly, histone deacetylases can also act as coactivators at a variety of genes.^{2,56-58} The tendency of PML/RAR α binding on open chromatin rather than compact chromatin¹⁴ strongly supports our findings. PML has been reported to exist in the PML/RAR α heterodimers/oligomers,⁵⁹⁻⁶¹ and P300 can interact with wild-type PML or PML/RAR α .^{62,63} It is deducible that P300 might interact with PML/RAR α either through PML within the PML-PML/RAR α oligomer or through the PML moiety of PML/RAR α . Whether an oligomerized PML/RAR α forms a complex with both P300 and HDAC1 simultaneously requires more evidence of future studies to support.

In addition to the newly identified role of transcriptional activation, we have also found that PML/RAR α , likely oligomerized, activates GFI1 through chromatin conformation at the super-enhancer region. This provides the structural basis for the efficient transcriptional activation. PML/RAR α could form oligomer via the RBCC domain,^{43,64} and this property enables PML/RAR α to interact with each other to regulate targets through the chromatin conformation in APL.

We note some limitations to our work, which was largely limited by available techniques. First, PML/RAR α target genes are identified through integrating RNA-seq (shRNA knockdown)

with ChIP-seq (against fusion site); such integration maximizes the power of each technique but cannot distinguish the regulation in a manner whether or not depending on DNA binding. Second, biochemical mechanisms of PML/RAR α action on chromatin looping to gene activation await investigation. Third, high-throughput assays are much needed to extensively validate PML/RAR α targets, especially activated targets. We anticipate that our work can be further extended with future technological innovations.

Finally, it is worth mentioning that small-molecule compounds selectively targeting super-enhancers have shown tremendous therapeutic potential in inhibiting cancer cell growth.⁶⁵ Inhibition of PML/RAR α -regulated super-enhancers, such as targeting GFI1 demonstrated in this study, may be one of the promising mechanisms that can be exploited pharmacologically to extend the success of ATRA/ATO therapy in APL.

Acknowledgments

The authors gratefully acknowledge the invaluable comments from Hugues de Thé (Université de Paris 7 Denis Diderot, Paris, France), the Center for High-Performance Computing at Shanghai Jiao Tong University for providing the computing platform, and Xujie Zhao for his helpful early inputs on this project.

H.F. is supported by the Program for Professor of Special Appointment (Eastern Scholar) at Shanghai Institutions of Higher Learning. This work was supported, in part, by the National Natural Science Foundation of China (grants 81530003, 81890994, and 81770153) and the National Key Research and Development Program (grant 2019YFA0905900).

Authorship

Contribution: K.W., Z.C., and Y.T. designed the experiments; Y.T., X.W., H.S., R.Z., Y.Z., and W.J. performed the experiments; Y.T., H.F., X.W., and S.L. analyzed the data; K.W. supervised the study and analysis; K.W., Y.T., and H.F. wrote the manuscript; Z.C. and S.C. gave conceptual advice; Z.C. revised the manuscript; and all authors discussed the results and implications and reviewed the manuscript.

Conflict-of-interest disclosure: The authors declare no competing financial interests.

ORCID profiles: Y.T., 0000-0001-8450-0392; X.W., 0000-0001-9767-6792; H.S., 0000-0001-6811-7844; Y.Z., 0000-0003-4861-5242; H.F., 0000-0003-3961-8572; K.W., 0000-0001-7198-2134.

Correspondence: Kankan Wang, Shanghai Institute of Hematology, State Key Laboratory of Medical Genomics, Ruijin Hospital Affiliated to Shanghai Jiao Tong University School of Medicine, 197 Ruijin Er Rd, Shanghai 200025, China; e-mail: kankanwang@shsmu.edu.cn; Zhu Chen, Shanghai Institute of Hematology, State Key Laboratory of Medical Genomics, Ruijin Hospital Affiliated to Shanghai Jiao Tong University School of Medicine, 197 Ruijin Er Rd, Shanghai 200025, China; e-mail: zchen@stn.sh.cn; and Hai Fang, Shanghai Institute of Hematology, State Key Laboratory of Medical Genomics, Ruijin Hospital Affiliated to Shanghai Jiao Tong University School of Medicine, 197 Ruijin Er Rd, Shanghai 200025, China; e-mail: hfang@well.ox.ac.uk.

Footnotes

Submitted 9 March 2020; accepted 20 August 2020; prepublished online on Blood First Edition 27 August 2020. DOI 10.1182/blood.2020005698.

*Y.T., X.W., and H.S. contributed equally to this study.

The data reported in this article have been deposited in the Gene Expression Omnibus database (accession numbers GSE126720 and GSE154269).

The online version of this article contains a data supplement.

There is a *Blood* Commentary on this article in this issue.

The publication costs of this article were defrayed in part by page charge payment. Therefore, and solely to indicate this fact, this article is hereby marked "advertisement" in accordance with 18 USC section 1734.

REFERENCES

- Bacher U, Schnittger S, Haeflrich T. Molecular genetics in acute myeloid leukemia. *Curr Opin Oncol*. 2010;22(6):646-655.
- Wang Z, Zang C, Cui K, et al. Genome-wide mapping of HATs and HDACs reveals distinct functions in active and inactive genes. *Cell*. 2009;138(5):1019-1031.
- de Thé H, Chen Z. Acute promyelocytic leukaemia: novel insights into the mechanisms of cure. *Nat Rev Cancer*. 2010;10(11):775-783.
- Wang K, Wang P, Shi J, et al. PML/RAR α targets promoter regions containing PU.1 consensus and RARE half sites in acute promyelocytic leukemia. *Cancer Cell*. 2010;17(2):186-197.
- Yang XW, Wang P, Liu JQ, et al. Coordinated regulation of the immunoproteasome subunits by PML/RAR α and PU.1 in acute promyelocytic leukemia. *Oncogene*. 2014;33(21):2700-2708.
- Wang ZY, Chen Z. Acute promyelocytic leukemia: from highly fatal to highly curable. *Blood*. 2008;111(5):2505-2515.
- Park DJ, Vuong PT, de Vos S, Douer D, Koeffler HP. Comparative analysis of genes regulated by PML/RAR α and PLZF/RAR α in response to retinoic acid using oligonucleotide arrays. *Blood*. 2003;102(10):3727-3736.
- Wartman LD, Welch JS, Uy GL, et al. Expression and function of PML-RARA in the hematopoietic progenitor cells of Ctg-PML-RARA mice. *PLoS One*. 2012;7(10):e46529.
- Yan J, Wang K, Dong L, et al. PML/RAR α fusion protein transactivates the tissue factor promoter through a GAGC-containing element without direct DNA association. *Proc Natl Acad Sci USA*. 2010;107(8):3716-3721.
- Coltella N, Percio S, Valsecchi R, et al. HIF factors cooperate with PML-RAR α to promote acute promyelocytic leukemia progression and relapse. *EMBO Mol Med*. 2014;6(5):640-650.
- Chen T, Dent SY. Chromatin modifiers and remodellers: regulators of cellular differentiation. *Nat Rev Genet*. 2014;15(2):93-106.
- Hnisz D, Abraham BJ, Lee TI, et al. Super-enhancers in the control of cell identity and disease. *Cell*. 2013;155(4):934-947.
- Ablain J, Leiva M, Peres L, Fonsart J, Anthony E, de Thé H. Uncoupling RARA transcriptional activation and degradation clarifies the bases for APL response to therapies. *J Exp Med*. 2013;210(4):647-653.
- Saeed S, Logie C, Francoijs KJ, et al. Chromatin accessibility, p300, and histone acetylation define PML-RAR α and AML1-ETO binding sites in acute myeloid leukemia. *Blood*. 2012;120(15):3058-3068.
- van der Meer LT, Jansen JH, van der Reijden BA. Gfi1 and Gfi1b: key regulators of hematopoiesis. *Leukemia*. 2010;24(11):1834-1843.
- Vassen L, Okayama T, Möry T. Gfi1b:green fluorescent protein knock-in mice reveal a dynamic expression pattern of Gfi1b during hematopoiesis that is largely complementary to Gfi1. *Blood*. 2007;109(6):2356-2364.
- Velinder M, Singer J, Bareyan D, et al. GFI1 functions in transcriptional control and cell fate determination require SNAG domain methylation to recruit LSD1 [published correction appears in *Biochem J*. 2017;474(17):2951]. *Biochem J*. 2016;473(19):3355-3369.
- Fraszczak J, Vadnais C, Rashkovan M, et al. Reduced expression but not deficiency of GFI1 causes a fatal myeloproliferative disease in mice. *Leukemia*. 2019;33(1):110-121.
- Hönes JM, Botezatu L, Helness A, et al. GFI1 as a novel prognostic and therapeutic factor for AML/MDS. *Leukemia*. 2016;30(6):1237-1245.
- Hönes JM, Thivakaran A, Botezatu L, et al. Enforced GFI1 expression impedes human and murine leukemic cell growth. *Sci Rep*. 2017;7(1):15720.
- Karsunky H, Zeng H, Schmidt T, et al. Inflammatory reactions and severe neutropenia in mice lacking the transcriptional repressor Gfi1. *Nat Genet*. 2002;30(3):295-300.
- Khandanpour C, Phelan JD, Vassen L, et al. Growth factor independence 1 antagonizes a p53-induced DNA damage response pathway in lymphoblastic leukemia. *Cancer Cell*. 2013;23(2):200-214.
- Marneth AE, Botezatu L, Hönes JM, et al. GFI1 is required for RUNX1/ETO positive acute myeloid leukemia. *Haematologica*. 2018;103(9):e395-e399.
- Zhang Y, Liu T, Meyer CA, et al. Model-based analysis of ChIP-Seq (MACS). *Genome Biol*. 2008;9(9):R137.
- Robinson MD, McCarthy DJ, Smyth GK. edgeR: a Bioconductor package for differential expression analysis of digital gene expression data. *Bioinformatics*. 2010;26(1):139-140.
- Martens JH, Brinkman AB, Simmer F, et al. PML-RAR α /RXR Alters the Epigenetic Landscape in Acute Promyelocytic Leukemia. *Cancer Cell*. 2010;17(2):173-185.
- Soignet SL, Maslak P, Wang ZG, et al. Complete remission after treatment of acute promyelocytic leukemia with arsenic trioxide. *N Engl J Med*. 1998;339(19):1341-1348.
- Ley TJ, Miller C, Ding L, et al; Cancer Genome Atlas Research Network. Genomic and epigenomic landscapes of adult de novo acute myeloid leukemia. *N Engl J Med*. 2013;368(22):2059-2074.
- Payton JE, Grieselhuber NR, Chang LW, et al. High throughput digital quantification of mRNA abundance in primary human acute myeloid leukemia samples. *J Clin Invest*. 2009;119(6):1714-1726.
- Rapin N, Bagger FO, Jendholm J, et al. Comparing cancer vs normal gene expression profiles identifies new disease entities and common transcriptional programs in AML patients. *Blood*. 2014;123(6):894-904.
- Bagger FO, Sasivarevic D, Sohi SH, et al. BloodSpot: a database of gene expression profiles and transcriptional programs for healthy and malignant haematopoiesis. *Nucleic Acids Res*. 2016;44(D1):D917-D924.
- Lübbert M, Hermann F, Koeffler HP. Expression and regulation of myeloid-specific genes in normal and leukemic myeloid cells. *Blood*. 1991;77(5):909-924.
- Luo H, Li Q, O'Neal J, Kreisel F, Le Beau MM, Tomasson MH. c-Myc rapidly induces acute myeloid leukemia in mice without evidence of lymphoma-associated antiapoptotic mutations. *Blood*. 2005;106(7):2452-2461.
- King-Underwood L, Pritchard-Jones K. Wilms' tumor (WT1) gene mutations occur mainly in acute myeloid leukemia and may confer drug resistance. *Blood*. 1998;91(8):2961-2968.
- Perissi V, Jepsen K, Glass CK, Rosenfeld MG. Deconstructing repression: evolving models of co-repressor action. *Nat Rev Genet*. 2010;11(2):109-123.
- Berger SL. The complex language of chromatin regulation during transcription. *Nature*. 2007;447(7143):407-412.
- Rahl PB, Lin CY, Seila AC, et al. c-Myc regulates transcriptional pause release. *Cell*. 2010;141(3):432-445.
- Wang T, Yu H, Hughes NW, et al. Gene essentiality profiling reveals gene networks and synthetic lethal interactions with oncogenic Ras. *Cell*. 2017;168(5):890-903.e815.
- Hock H, Hamblen MJ, Rooke HM, et al. Gfi-1 restricts proliferation and preserves functional integrity of hematopoietic stem cells. *Nature*. 2004;431(7011):1002-1007.
- Pokorna K, Le Pogam C, Chopin M, et al. Tracking the extramedullary PML-RAR α -positive cell reservoirs in a preclinical model: biomarker of long-term drug efficacy. *Mol Cell Probes*. 2013;27(1):1-5.
- Zhang XW, Yan XJ, Zhou ZR, et al. Arsenic trioxide controls the fate of the PML-RAR α oncoprotein by directly binding PML. *Science*. 2010;328(5975):240-243.
- Simonis M, Kooren J, de Laat W. An evaluation of 3C-based methods to capture DNA interactions. *Nat Methods*. 2007;4(11):895-901.
- Li Y, Ma X, Chen Z, et al. B1 oligomerization regulates PML nuclear body biogenesis and leukemogenesis. *Nat Commun*. 2019;10(1):3789.

44. Gilbert LA, Larson MH, Morsut L, et al. CRISPR-mediated modular RNA-guided regulation of transcription in eukaryotes. *Cell*. 2013;154(2):442-451.
45. Singh AA, Mandoli A, Prange KH, Laakso M, Martens JH. AML associated oncofusion proteins PML-RARA, AML1-ETO and CBFB-MYH11 target RUNX/ETS-factor binding sites to modulate H3ac levels and drive leukemogenesis. *Oncotarget*. 2017;8(8):12855-12865.
46. Martens JH, Mandoli A, Simmer F, et al. ERG and FLI1 binding sites demarcate targets for aberrant epigenetic regulation by AML1-ETO in acute myeloid leukemia. *Blood*. 2012; 120(19):4038-4048.
47. Shivdasani RA, Orkin SH. The transcriptional control of hematopoiesis. *Blood*. 1996;87(10): 4025-4039.
48. Thambyrajah R, Mazan M, Patel R, et al. GFI1 proteins orchestrate the emergence of haematopoietic stem cells through recruitment of LSD1. *Nat Cell Biol*. 2016;18(1):21-32.
49. Hock H, Hamblen MJ, Rooke HM, et al. Intrinsic requirement for zinc finger transcription factor Gfi-1 in neutrophil differentiation. *Immunity*. 2003;18(1):109-120.
50. Horman SR, Velu CS, Chaubey A, et al. Gfi1 integrates progenitor versus granulocytic transcriptional programming. *Blood*. 2009; 113(22):5466-5475.
51. Jeanne M, Lallemand-Breitenbach V, Ferhi O, et al. PML/RARA oxidation and arsenic binding initiate the antileukemia response of As2O3. *Cancer Cell*. 2010;18(1):88-98.
52. Nasr R, Guillemain MC, Ferhi O, et al. Eradication of acute promyelocytic leukemia-initiating cells through PML-RARA degradation [published correction appears in *Nat Med*. 2008;15:117]. *Nat Med*. 2008;14(12): 1333-1342.
53. Yoshida H, Kitamura K, Tanaka K, et al. Accelerated degradation of PML-retinoic acid receptor alpha (PML-RARA) oncoprotein by all-trans-retinoic acid in acute promyelocytic leukemia: possible role of the proteasome pathway. *Cancer Res*. 1996;56(13):2945-2948.
54. Carrozza MJ, Li B, Florens L, et al. Histone H3 methylation by Set2 directs deacetylation of coding regions by Rpd3S to suppress spurious intragenic transcription. *Cell*. 2005;123(4): 581-592.
55. Tiana M, Acosta-Iborra B, Puente-Santamaría L, et al. The SIN3A histone deacetylase complex is required for a complete transcriptional response to hypoxia. *Nucleic Acids Res*. 2018;46(1):120-133.
56. Greer CB, Tanaka Y, Kim YJ, et al. Histone deacetylases positively regulate transcription through the elongation machinery. *Cell Rep*. 2015;13(7):1444-1455.
57. Benesch MA, Segala G, Wider D, Picard D. LSD1 engages a corepressor complex for the activation of the estrogen receptor α by estrogen and cAMP. *Nucleic Acids Res*. 2016; 44(18):8655-8670.
58. Marié IJ, Chang HM, Levy DE. HDAC stimulates gene expression through BRD4 availability in response to IFN and in interferonopathies. *J Exp Med*. 2018;215(12): 3194-3212.
59. Kastner P, Perez A, Lutz Y, et al. Structure, localization and transcriptional properties of two classes of retinoic acid receptor alpha fusion proteins in acute promyelocytic leukemia (APL): structural similarities with a new family of oncoproteins. *EMBO J*. 1992;11(2): 629-642.
60. Perez A, Kastner P, Sethi S, Lutz Y, Reibel C, Chambon P. PMLRAR homodimers: distinct DNA binding properties and heteromeric interactions with RXR. *EMBO J*. 1993;12(8): 3171-3182.
61. Dyck JA, Maul GG, Miller WH Jr., Chen JD, Kakizuka A, Evans RM. A novel macromolecular structure is a target of the promyelocyte-retinoic acid receptor oncoprotein. *Cell*. 1994; 76(2):333-343.
62. Hayakawa F, Abe A, Kitabayashi I, Pandolfi PP, Naoe T. Acetylation of PML is involved in histone deacetylase inhibitor-mediated apoptosis. *J Biol Chem*. 2008;283(36): 24420-24425.
63. Yoshida H, Ichikawa H, Tagata Y, et al. PML-retinoic acid receptor alpha inhibits PML IV enhancement of PU.1-induced C/EBPepsilon expression in myeloid differentiation. *Mol Cell Biol*. 2007;27(16):5819-5834.
64. Wang P, Benhenda S, Wu H, et al. RING tetramerization is required for nuclear body biogenesis and PML sumoylation [published correction appears in *Nat Commun*. 2018;9: 1841]. *Nat Commun*. 2018;9(1):1277.
65. Christensen CL, Kwiatkowski N, Abraham BJ, et al. Targeting transcriptional additions in small cell lung cancer with a covalent CDK7 inhibitor [published correction appears in *Cancer Cell* 2015;27(1):149]. *Cancer Cell*. 2014;26(6):909-922.